

Received March 7, 2018, accepted April 10, 2018, date of publication April 20, 2018, date of current version May 16, 2018.

Digital Object Identifier 10.1109/ACCESS.2018.2828830

# No-Reference Contrast Measurement for Color Images Based on Visual Stimulus

MINSUB KIM<sup>1</sup>, KI SUN SONG, AND MOON GI KANG

School of Electrical and Electronic Engineering, Yonsei University, Seoul 03722, South Korea

Corresponding author: Moon Gi Kang (mkang@yonsei.ac.kr)

This research was supported by Basic Science Research Program through the National Research Foundation of Korea (NRF) funded by the Ministry of Science, ICT and Future Planning (2015R1A2A1A14000912).

**ABSTRACT** Image quality assessment without a reference image is essential for evaluating the performance of image enhancements. Much research has been done to develop an objective image quality measurement that is relevant to perceived quality evaluations. Because the contrast of an image is one of the important factors for a user to evaluate the image quality, methods for improving the contrast of images are also being extensively studied, but the assessment algorithms for evaluating them are limited. In this paper, we propose a contrast measurement of a color image based on a stimulus in the human visual system (HVS). The proposed method evaluates the luminance component of the image based on just-noticeable-difference to reflect the local contrast perceived in the HVS. The contrast in the color component is evaluated based on a model of the stimulus of the color component in the primary visual cortex (V1). The region response factor, which reflects the relative change of the color saturation in the different luminance values in V1, is used to image contrast. We tested the validity of the proposed method using various image databases and subjective tests. The experimental results showed that the proposed method had higher correlation with the evaluation of people than conventional methods of measuring image contrast without the original image.

**INDEX TERMS** Image quality assessment, image contrast measurement, human visual system, no-reference, color image.

## I. INTRODUCTION

With the development in imaging technology, acquiring digital images has become easier for people by using digital devices such as digital cameras and smart phones. Because the demands of people for high quality images continue to increase, the images thus obtained are provided to the users with improved quality through various enhancement algorithms. Therefore, image quality assessment (IQA), which means evaluation of the objective quality of the images, becomes a key role in image processing. This quality assessment can be considered as deciding the quality of an image. High quality images can be defined as images with low distortion and high contrast. Image distortion means that the original image is degraded by blur, noise, compression artifact, etc. during the image acquisition process. The best measurement method of the image quality presented above is to measure all the preferences of people on the image. This method is called subjective IQA. The mean of the people preferences measured in this manner is called the mean of opinion score (MOS). An image with high MOS can be considered to

be accepted by people as a good image. In practice, however, measuring the subjective evaluation of people of every image is very difficult in terms of money and time.

To solve these problems, many algorithms have been developed to measure the image quality without subjective evaluations. These measurement algorithms are called objective IQA algorithms. Because they have a high correlation with the quality of the images that people actually evaluate, the perceptual quality of a given image can be measured using objective IQA algorithms. These objective IQA algorithms are classified into three types depending on the presence or absence of the original image [1]. The three categories are full-reference (FR), reduced-reference (RR), and no-reference (NR) methods. The popular algorithms are peak signal to noise ratio (PSNR) [2], structural similarity index measure (SSIM) [3], [4] and using the machine learning [5], or the neural network [6]. In practical applications, for example, in image enhancement or capture, the original image cannot always be available, and therefore, a large number of NR IQA methods are required.

Whereas the contrast of an image cannot be determined as a distortion factor, it is an important factor that determines the image quality [7]. One example is that the features present in a good contrast image are more distinguishable than those present in a bad contrast image. Various enhancement methods have been studied, from histogram equalization to the recently published algorithms, to improve the contrast of images reduced by various natural environments [8], [9]. Considering the image before the enhancement as a reference image is hard to assume because the fidelity between them is not important. Therefore, an NR approach is required for images with improved contrast. Using this method, we can measure the image quality without obtaining MOS and determine the suitability of the enhancement method.

Two methods are available for measuring the contrast of an image without a reference image. One is the natural scene statistics (NSS) method, which measures the quality of images by measuring how natural the images are. The other is to model the human visual system (HVS) and measure the image quality taking into account how a person accepts the image. On the basis of NSS, several assessment algorithms are available to measure the image contrast without a reference [10], [11]. The other model, i.e., HVS model, analyzes how the image acts as a stimulus through HVS. This HVS based measurement method is based on Michelson contrast [12] and Weber's law [13]. Since then, several methods have been presented to incorporate HVS studies into the image contrast [14]–[16].

However, the existing methods have certain limitations. Because the NSS based method measures the quality of an image under the assumption that the naturalness of the image changes when the image is distorted/enhanced, a lack of consideration exists on how people determine the image. For this reason, a model for determining the image contrast in HVS should be established to measure the contrast of the image in order to determine how the user evaluates the image contrast. In addition, a model which includes not only the measurement of grayscale images, but also the relationship between the image brightness and color components is needed to evaluate a color image.

Much research has been studied on how contrast of color component received from the visual system to the human brain. These studies modeled how contrast of color component accepted to human brain through neuroscientists experiments. In the beginning, Hurvich and Jameson [17] proposed that the image information received from the visual cortex is shifted to the primary visual cortex (V1) part of the brain separately by the luminance and color components, and processed by V1. Johnson *et al.* [18] proposed that color and brightness contrast interact at V1. Xing *et al.* [19] found that as luminance contrast increased, when either the surround luminance increases or decreases, the apparent color saturation of the target gradually decreased. It is proved through psychophysics experiment and changes of visual evoked potential.

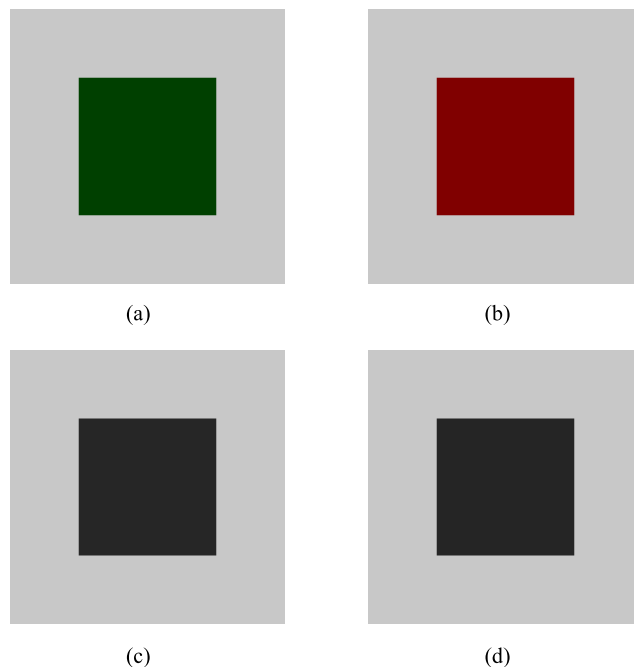


**FIGURE 1.** Different color images with the same grayscale. (a) and (b) two different color patches. (c) and (d) luminance component of each color patch.

Fig. 1 shows an example in which two different patches have the same grayscale image. In this example, luminance component is used as a grayscale image. Because the luminance values of the two images are the same as shown in Figs. 1 (c) and (d), we can see the limitation that the difference between the two images cannot be distinguished by the conventional methods of contrast measurement.

In this paper, we propose a new NR IQA method to measure the contrast of color images. The proposed method uses the HVS property in which the visibility threshold of the local region changes according to the average value of the region [20], and the local region contrast factor is calculated by obtaining the region adaptive visibility threshold. Further, whereas the conventional methods use only the luminance component of the image to measure the image contrast, the proposed method converts the image into another color difference domain to distinguish the image contrast, which could not be distinguished using the luminance component. Through this process, we can possibly measure the contrast of a color image similar to actual evaluation by people.

The rest of this paper is organized as follows. Section 2 reviews the conventional contrast measurement, including the NR contrast measurement based on HVS. Section 3 proposes a new algorithm to measure the contrast of a color image. Section 4 presents the experimental results and comparisons with the conventional methods using MOS. The conclusions are discussed in Section 5.

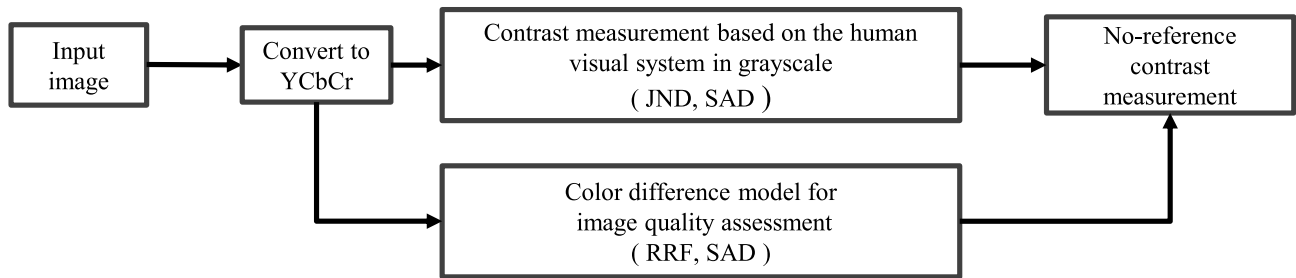


FIGURE 2. Block diagram of the proposed method.

## II. RELATED WORK

Conventional NR IQA algorithms use the mathematical distribution of an image to measure its contrast. In particular, these methods are used for measurement and enhancement of the local contrast of an image, for example, its average, variance, or entropy. These mathematical based measurements do not provide people opinion of images because they actually measure the contrast of an image using its global and local statistical characteristic. Morrow *et al.* [21] proposed a method for evaluating the contrast of an image using contrast histogram, which has much more consistency than the methods that use existing mathematical features. Several measurements using a contrast measurement for image enhancement have been developed following this observation. These methods measure the image quality based on HVS as a method of measuring the image contrast that a human actually receives.

Using the Weber's law mentioned in Sec. I, many methods of measuring the contrast of an image to measure the local contrast have been proposed. Agaian proposed the measurement of enhancement (EME) and measure of enhancement by entropy (EMEE) based on Weber's law [14]. Panetta *et al.* [15] proposed root mean enhancement (RME), which measures the degree of enhancement of images using both HVS and root mean square (RMS) contrast concepts.

The methods for measuring the image contrast mentioned above are contrast measurements for grayscale images; thus it is difficult to apply to color images. Most of the conventional methods convert a color image to a grayscale image when evaluating the contrast. Panneta *et al.* [16] proposed a method to obtain a grayscale image that considers the correlation of each channel using HVS to convert the color image to grayscale. In addition, to measure the contrast of each color channel, Panneta *et al.* [15] proposed the color/cube RME (CRME), which applies the concept of RME to color images. Rizzi *et al.* [22] and [23] proposed a method of measuring the contrast of color images in the CIELab color domain using the method from measure the contrast of images in grayscale and the difference of gaussian (DOG). In the above mentioned methods, the contrast of the whole image is measured in the same way regardless of the color channel or color domain. These methods measure the contrast based on HVS, but because the contrast of the image is measured for the same way, each channel property cannot be considered. In the

proposed method, different models for the luminance and color difference domains are used to measure the contrast of a color image. The color image contrast is measured in a similar manner to that of the human senses using the HVS feature where the response of the chrominance components is different depending on the background luminance of the image.

## III. PROPOSED METHOD

In the proposed method, a contrast measurement based on HVS is proposed for color image. The color image contrast of the luminance component is measured using the just-noticeable-difference (JND), which is a threshold value where people feel the difference between two stimuli. The luminance component, which is used in this paper, can be expressed as

$$L = 0.299 \cdot R + 0.587 \cdot G + 0.114 \cdot B, \quad (1)$$

where  $R$ ,  $G$ , and  $B$  mean the red, green, and blue channel intensity, respectively, based on the fact that the amount of acceptance in HVS is different for each channel [16]. In addition, to compensate the limitation of the measurement in the luminance domain, the proposed method calculates the image contrast using the color difference domain. Through these methods, calculating the contrast based on the HVS is possible. Fig. 2 shows the block diagram of the proposed method. Fig. 2 shows that the image is separated into the luminance and the color difference components, and each image contrast is measured. The color image contrast is finally obtained using these factors.

### A. CONTRAST MEASUREMENT BASED ON HVS IN GRAYSCALE

In the proposed method, the contrast of the image in grayscale is first obtained. When the input image is separated into the luminance and color components, the luminance component is used to measure the local contrast of the corresponding image in grayscale. In a real image, the background luminance of the image affects the contrast. Therefore, limitation exists in using the Weber's law on the luminance component [24]. We measure the visibility threshold of the local region based on the background luminance to overcome this limitation. The visibility threshold of the region changes

according to the background luminance of the local region in the image. The measurement of the visibility threshold of the local area uses the model proposed by Chou and Li [20]. JND can be expressed as

$$JND(k) = \begin{cases} T_0[1 - (\frac{k}{127})^\lambda] + 3, & k \leq 127 \\ \gamma(k - 127) + 3, & \text{otherwise,} \end{cases} \quad (2)$$

where  $T_0, \gamma$ , and  $\lambda$  are constants and  $k$  is local region background luminance. In a standard 8-bit image,  $T_0, \gamma$ , and  $\lambda$  are 17,  $3/128$ , and 0.5, respectively. From (2), the visibility threshold decreases as the background luminance increases when the background luminance is smaller than 127. When the background luminance is larger than 127, the visibility threshold value increases as the background luminance increases. Thus, the visibility threshold changes with the background luminance value. Because the average value of the local region affects the local contrast, in this paper, the visibility threshold is obtained using the average value of the local region. The visibility threshold of the luminance component can be expressed as

$$Th_{(i,j)} = JND(\bar{I}_{(i,j)}), \quad (3)$$

and

$$\bar{I}_{(i,j)} = \frac{1}{mn} \sum_{p=-\frac{m}{2}}^{\frac{m}{2}} \sum_{q=-\frac{n}{2}}^{\frac{n}{2}} I_{i+p,j+q}, \quad (4)$$

where  $\bar{I}_{(i,j)}$  denotes the average intensity of the luminance and  $m$  and  $n$  denote the vertical and horizontal mask size, respectively, of the local region.  $I_{i+p,j+q}$  denotes the intensity of the pixels in the local region, which is centered at  $(i, j)$ .  $Th_{(i,j)}$  denotes the local region visibility threshold, which is calculated by (2).

The local contrast of the luminance image is measured using  $Th_{(i,j)}$ . First, using the visibility threshold, the relationship between the pixels of the local region and the visibility threshold is calculated, which is defined as the local contrast factor. The local contrast factor is expressed as the product of two terms that determine the degree of contrast of each local region and how much of its contrast satisfies the visibility threshold for each block. The local contrast factor can be expressed as

$$C_{(i,j)} = SAD_{(i,j)} \cdot FJND_{(i,j)}, \quad (5)$$

where  $C_{(i,j)}$  is the local contrast factor of the local region centered at  $(i, j)$ . The local contrast factor is expressed as the product of  $SAD_{(i,j)}$ , which is the average of the absolute difference in each region and  $FJND_{(i,j)}$ , which is the degree that satisfies the visibility threshold. These factors can be expressed as

$$SAD_{(i,j)} = \frac{1}{mn} \left( \sum_{p=-\frac{m}{2}}^{\frac{m}{2}} \sum_{q=-\frac{n}{2}}^{\frac{n}{2}} |I_{i+p,j+q} - \bar{I}_{(i,j)}| \right), \quad (6)$$

and

$$FJND_{(i,j)} = \frac{(\max - \min)^\tau}{Th_{(i,j)}}. \quad (7)$$

To measure the contrast factor of each local region,  $SAD_{(i,j)}$  calculates how much each pixel in the region differs from the average values in the same region, and  $FJND_{(i,j)}$  calculates how much each region satisfies the visibility threshold. By multiplying these two terms, we can measure how well the local region contrast satisfies HVS. In (7),  $\max$  and  $\min$  denote the local maximum and minimum of the local area centered on  $(i, j)$ .  $\tau$  is a factor that applies the weight to the difference between  $\max$  and  $\min$ . In measuring the contrast factor of the local area, the larger the value of  $SAD_{(i,j)}$  is, the greater is the estimated contrast of the local area. Further, from the value of  $FJND_{(i,j)}$ , we can evaluate whether the difference between the maximum and minimum values in the region satisfies the visibility threshold according to the relationship with visibility threshold  $Th_{(i,j)}$ . If the difference between the maximum and minimum values of the area is larger than the visibility threshold, it is evaluated that the visibility threshold is satisfied. Through this process, the proposed method can measure the contrast of the local region terms of HVS.

$C_{(i,j)}$  depends on the change in the values of  $m$  and  $n$ , which determine the size of the local area. The contrast of the entire image of the luminance component is measured using the average contrast factor of the local area obtained by adjusting the mask size. The contrast of the luminance component is defined as

$$C_L = \frac{1}{(M \cdot N)} \sum_{i=0}^{M-1} \sum_{j=0}^{N-1} C_{(i,j)}, \quad (8)$$

where,  $M$ , and  $N$  denote the numbers of rows and columns of the input image, respectively.

## B. COLOR DIFFERENCE MODEL FOR CONTRAST MEASUREMENT

From the contrast measurement method proposed in Sec. III-A, the contrast based on HVS can be measured using the luminance component. In most cases, the quality of an image can be measured using only the luminance component of the image, as presented in Sec. III-A. However, some cases exist where the contrast of different images cannot be distinguished by the luminance component. When the image is converted into the luminance domain, a situation occurs in which the luminance components are the same even when the images have different colors.

We propose a method to measure the image quality using the color difference domain to solve this problem. Because the color components of an image that constitute the luminance are different, the image contrast can be calculated for images with the same luminance when the image contrast is measured in the color difference domain. In addition, because the color information also affects the contrast of a color image, the difference in the color component can be used as

an indicator to measure the image contrast by the relationship in the color domain. The saturation of the color image in HSI color space can be expressed as

$$S = \frac{I - a}{I} \quad \text{where } a = \min[(R, G, B)], \quad (9)$$

where  $S$  is the saturation of the image. Equation (9) indicates that when the intensity of the image increases, the saturation of the image decreases. Thus, people feel that the color contrast changes when contrast enhancement is applied to a normal image. We can see from this example that the contrast affected by the color components that make up the image. However, (9) can only explain the increase or decrease in the image saturation in the enhancement of the image, but explanation on how this change actually affects the human acceptance is lacking. Further, because we measure the contrast of the color component of the image in the absence of a reference image, we need a model on how we perceive the change in the color component in HVS.

To model the acceptance of a color image in HVS, we separate the color component into two parts: intensity and saturation. For the color component intensity, we use  $SAD_{(i,j)}$  which is the same method used in the luminance component.  $SAD_{(i,j)}$  is used to evaluate whether an intensity difference exists or does not. If an intensity difference exists in color difference domain, a color difference exists. The other component is color saturation. As mentioned above, saturation is an important component for people to measure the contrast. To measure the degree of image's saturation on the contrast, we use a model that determines how the color contrast is received from the visual system to the human brain based on previous studies [18], [19].

Fig. 3 shows an example of the relationship between the color contrast and luminance. In Fig. 3, each color patch (green, red) has the same intensity. However, depending on the brightness, the contrast in the relative color patches is different. The brightness values in each row are 30, 200, and 230, and the intensity of the two color patches is 200. Because patches in Figs. 3 (c) and (d) have same intensity with surroundings, the relative saturation is the smallest for these patches. The overall contrast for the local patch is different from the saturation. The overall contrast of the color patches is the highest for Figs. 3 (a) and (b) because of the intensity and saturation difference. To consider this condition, we measure the region response factor (RRF) of the saturation in each region and calculate the contrast factor according to the region brightness.  $RRF$  can be expressed as

$$RRF_{(i,j)} = \begin{cases} \left(\frac{\bar{I} - \psi(i,j)}{\psi(i,j)}\right)^\eta + v_{off}, & \text{if } \bar{I} \geq \psi(i,j) \\ \left(\frac{\psi(i,j) - \bar{I}}{\psi(i,j)}\right)^\eta + v_{off}, & \text{otherwise,} \end{cases} \quad (10)$$

where  $\psi(i,j)$  is the brightness value of the corresponding region centered at  $(i,j)$ ,  $\eta$  is the weight factor, and  $v_{off}$  is the offset value. The mask size of  $\psi(i,j)$  is usually two times

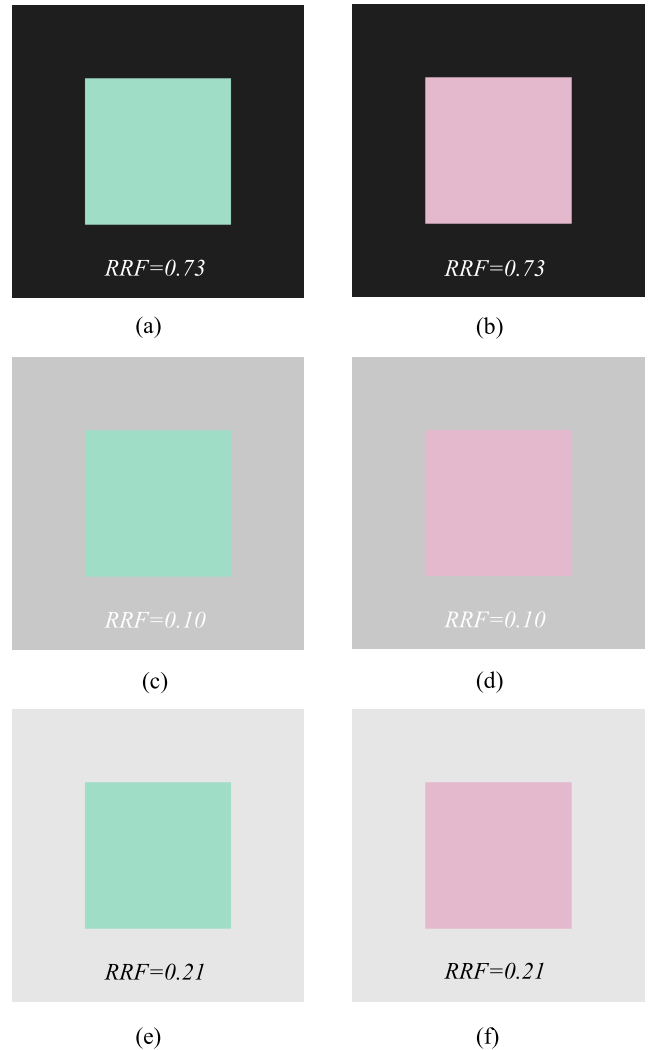


**FIGURE 3. Relationship between brightness and color contrast. (a) and (b) color patch with brightness of 30. (c) and (d) color patch with brightness of 200. (e) and (f) color patch with brightness of 230.**

larger than that of  $\bar{I}$ . In the proposed method, the luminance value of the area is used to obtain the brightness value.  $v_{off}$  is the offset value for when  $\bar{I}$  and  $\psi(i,j)$  are equal. It prevents the contrast of the image from being estimated as 0. Fig. 4 shows the  $RRF$  graph when  $\psi = 30$ , which shows that the  $RRF$  value can be changed by changing the  $\eta$ . The value of  $\eta$  which is highly correlated to the actual evaluation, is determined by changing its value, and 1 is used as the value of  $\eta$ .

By using this  $RRF$ , the relationship between the saturation and brightness can be defined. The  $RRF$  value can be changed by  $\psi(i,j)$ , which represents the brightness of the region. Fig. 5 shows the graph of the  $RRF$  for Fig. 3. Fig. 4 and Fig. 5 show the region adaptivity of the  $RRF$ .

Fig. 3 shows that  $RRF$  is the smallest in Figs. 3 (c) and (d). The  $RRF$  is the same for the green and red patches because the two patches have the same brightness. In addition, according to the HVS response to the saturation, the  $RRF$  decreases as

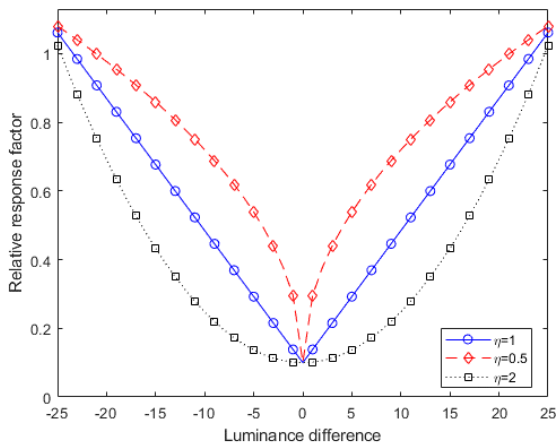


FIGURE 4. Graph of RRF for  $\psi = 30$ .

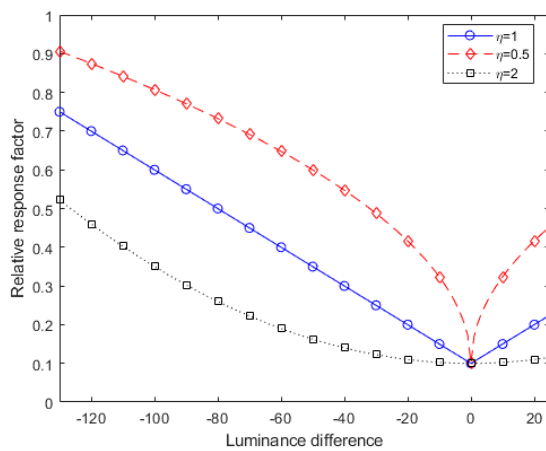


FIGURE 5. Graph of RRF for Fig. 3.

the difference between the brightness and luminance values decreases. To calculate the color contrast of the image, various domains such as YCbCr, YUV, and YIQ can be used. The proposed method uses the  $Cb$  and  $Cr$  domains as the chrominance domain.

Considering these differences and the above mentioned saturation and brightness contrast, the contrast in the color difference domain is measured as follows. First, a mathematical contrast measurement algorithm is used to measure the presence or absence of chrominance components.  $SAD_{(i,j)}$  described in Sec. III-A is used as the measurement method. It calculates the average of the absolute value of the difference between the average value of the area and the pixel value existing in the area. If the  $SAD_{(i,j)}$  value is large, we can consider that the corresponding region contains many different color components. After measuring the different color components contained in the area, we use  $RRF$  and calculate how the saturation of the area is affected by the brightness. The final contrast measurement equations for the  $Cb$  and  $Cr$

domains can be expressed as

$$C_{Cb,Cr} = \frac{1}{MN} \sum_{i=0}^{M-1} \sum_{j=0}^{N-1} \times \left( RRF_{(i,j)} \cdot \left( \frac{1}{mn} \sum_{p=-r}^r \sum_{q=-s}^s |I_{i+p,j+q} - \bar{I}| \right) \right). \quad (11)$$

The final equation of the image contrast that considers the color difference domain can be expressed as

$$C_{Image} = [C_L]^\alpha \cdot [C_{Cb}]^\beta \cdot [C_{Cr}]^\theta, \quad \text{subject to } \alpha + \beta + \theta = 1. \quad (12)$$

In (12),  $C_L$  denotes the quality value calculated using the luminance component of the image presented in Sec. III-A, and  $C_{Cb}$  and  $C_{Cr}$  represent the qualities calculated using the color difference domain component of the image presented in Sec. III-B.  $\alpha$ ,  $\beta$ , and  $\theta$  are the weights of the respective components. Table 1 lists the proposed contrast measurement of Fig 3.

The contrast of each component and the overall contrast are listed in Table 1. For Figs. 3 (c) and (d), the luminance components are equal for the background luminance; thus, the luminance contrast is 0. Figs. 3 (a) and (b), and Figs. 3 (c) and (d) also have the same contrast in the luminance domain, because the patches located in the same row have the same luminance value with different colors. Using the proposed method in the color difference domain, contrast of Fig. 3 can be evaluated. In the measurements in the  $Cb$  and  $Cr$  domains, the patches located in the same row show different contrast values. Further, with regard to the color components, each column has similar contrast values for the  $Cb$  and  $Cr$  components. This result indicates that the contrast difference for that shown in Fig. 3 occurs from not only the luminance but also the saturation. The overall contrast measurement is the highest for Figs. 3 (a) and (b) and lowest for Figs. 3 (c) and (d), which fits how people evaluate these ideal images.

## IV. EXPERIMENTAL RESULTS

### A. DATABASE DESCRIPTION

In this section, we present the validation of our proposed method using different image databases. We evaluate the validity of the proposed method by selecting a database containing a change in contrast among several different image databases. The selected image databases are TID2008 [25], TID2013 [26], CSIQ [27], and CCID2014 [28]. Here, we briefly describe the selected image databases. First, the TID2008 database is designed to measure color image quality. It consists of 25 reference images and 17 distorted images. The TID2013 database is an extended version of TID2008 and contains the largest number of images in the existing image database. TID2013 contains 24 distorted images of the 25 original images. Because the proposed

**TABLE 1.** Contrast measurement on the color difference domain of Fig. 3.

	Fig.3 (a)	Fig.3 (b)	Fig.3 (c)	Fig.3 (d)	Fig.3 (e)	Fig.3 (f)
$C_L$ (Contrast on luminance domain)	21.5	21.5	0.00	0.00	14.29	14.29
$C_{Cb}$ (Contrast on $Cb$ domain)	1.40	0.96	1.38	0.95	1.40	0.96
$C_{Cr}$ (Contrast on $Cr$ domain)	0.33	1.32	0.32	1.30	0.33	1.29
$C_{Image}$ (Overall image contrast)	5.44	8.09	0.12	0.55	4.07	7.42

**FIGURE 6.** Example of the contrast change in the TID2013 dataset.

method measures the image contrast, only the change set of the contrast changes in the two databases is used. Fig. 6 shows an example of the contrast change in the TID2013set.

CSIQ includes 30 original images and 6 types of distorted images. We used only 116 images with changes in the contrast in the test. Finally, the CCID2014 database is created using only images with different contrasts. CCID2014 consists of 15 reference images and 655 images with contrast changes due to gamma transfer and concave function. These databases also provides MOS or differential mean opinion score (DMOS) for each image. MOS is evaluated using the score by people within suitable viewing distance and illuminance according to the International Telecommunication Union guideline (ITU-R BT.500-13) [29]. From this process, we can obtain the evaluations of each image by the people. In case of MOS, the higher the score is, the better is the image evaluation by people because it gives a low score to a bad image. In contrast to MOS, in the case of DMOS, the difference among images evaluation is obtained. Therefore, the larger the DMOS value is, the worse is the image evaluation.

## B. PERFORMANCE EVALUATION OF THE DATABASES

To verify the performance of the proposed method, we compare the results of the existing method with the database set. For each database, three correlation factors are used to evaluate how each algorithm is highly related to HVS. The three correlation factors are Pearson linear correlation coefficient (PLCC) [30], Spearman rank order correlation coefficient (SRCC) [31], and Kendall rank order correlation coefficient (KRCC) [32]. PLCC measures the degree of the objective score and the MOS/DMOS changes together. SRCC

is a rank based measurement that measures the degree of relationship between two values using rank, instead of data values. Finally, KRCC measures the ratio of each rank to non normal data. In the case of the objective quality assessment algorithm, it can be considered as a replacement of the subjective quality assessment when it has a high correlation with MOS.

The comparison of the proposed method is performed using different NR contrast measurement algorithms. The comparison algorithms can be roughly divided into three types. The first type includes RMS, RME, and RAMMG, which are based on HVS and measure the contrast of images in grayscale. The second type includes the DIQM, CRME, and RSC methods to measure the contrast of HVS based color images. Finally, blind/referenceless image spatial quality evaluator (BRISQUE) and natural image quality evaluator (NIQE) [33] are used to measure the image contrast based on NSS.

We used a  $3 \times 3$  mask for local mask sizes  $m$  and  $n$  in the proposed method. The parameter for local contrast factor  $\tau$  is set to 1. The proposed method for the luminance component is multi-scalable. We only used a single scale, namely,  $3 \times 3$ , for experiment because other comparison algorithms are usually not multi-scalable. For the contrast measurement of the color images, we set  $\eta$  as 1. The three parameters for the final image quality, namely,  $\alpha$ ,  $\beta$  and  $\theta$ , are set to 0.8, 0.1, and 0.1, respectively. These parameters have been set up using optimized parameters that are most correlated with people's evaluation through various experiments. To optimize these parameters, we use the parameters with the highest correlation value to the databases mentioned in IV-A and IV-C while changing the values of the parameters to 0.05.

Table 2 lists the comparison algorithms for each database and the correlation factor of the proposed method. The results of the proposed method and those of the algorithm with the highest numerical value are shown in bold. Because the proposed method measures both the grayscale and color images, both experimental results are also included. These results are denoted by luminance only and color model respectively.

First, we can see that the proposed method for PLCC has the highest value in the existing comparison algorithms. This result suggests that the proposed method has the most similar degree of change to MOS/DMOS. In the case of SRCC, it indicates how well each algorithm follows the rank based on the rank of the image set. The list in Table 3 shows that SRCC differs according to the image database. The SRCC values

TABLE 2. PLCC of the algorithms using different datasets.

	TID2008	TID2013	CSIQ	CCID2014
RMS	0.9336	0.9084	0.8786	0.9333
RME	0.9605	0.9439	0.8542	0.9605
RAMMG	0.9554	0.9257	<b>0.8826</b>	0.9554
DIQM	<b>0.9632</b>	0.9504	0.8298	<b>0.9632</b>
CRME	0.9569	<b>0.9489</b>	0.8356	0.9569
RSC	0.3505	0.2760	0.1899	0.3505
BRISQUE	0.0985	0.1011	0.1083	0.5514
NIQE	0.2366	0.2068	0.3079	0.2849
P.M.(luminance only)	<b>0.9677</b>	<b>0.9578</b>	<b>0.8867</b>	<b>0.9646</b>
P.M.(color model)	<b>0.9656</b>	<b>0.9556</b>	<b>0.8845</b>	<b>0.9564</b>

TABLE 3. SRCC of the algorithms using different datasets.

	TID2008	TID2013	CSIQ	CCID2014
RMS	<b>0.8459</b>	<b>0.8848</b>	<b>1.0000</b>	<b>0.8459</b>
RME	0.8000	<b>0.8848</b>	<b>1.0000</b>	<b>0.8459</b>
RAMMG	0.8000	<b>0.8848</b>	<b>1.0000</b>	0.8000
DIQM	<b>0.8459</b>	<b>0.8848</b>	<b>1.0000</b>	0.8459
CRME	0.8333	<b>0.8848</b>	<b>1.0000</b>	0.8333
RSC	0.4333	0.1923	0.093	0.4333
BRISQUE	0.0985	0.0379	0.600	0.5514
NIQE	0.2366	0.2421	0.1083	0.2849
P.M.(luminance only)	<b>0.8459</b>	<b>0.8848</b>	<b>1.0000</b>	<b>0.8459</b>
P.M.(color model)	<b>0.8459</b>	<b>0.8848</b>	<b>1.0000</b>	<b>0.8459</b>

TABLE 4. KRCC of the algorithms using different datasets.

	TID2008	TID2013	CSIQ	CCID2014
RMS	<b>0.7565</b>	<b>0.8135</b>	<b>0.0333</b>	0.1371
RME	<b>0.7565</b>	<b>0.8135</b>	<b>0.0333</b>	0.2726
RAMMG	<b>0.7565</b>	<b>0.8135</b>	<b>0.0333</b>	<b>0.3918</b>
DIQM	<b>0.7565</b>	<b>0.8135</b>	<b>0.0333</b>	0.2969
CRME	<b>0.7565</b>	<b>0.8135</b>	<b>0.0333</b>	0.3168
RSC	0.3686	0.0682	0.0111	0.1692
BRISQUE	0.0365	0.0509	0.0111	0.2696
NIQE	0.2302	0.2594	0.0222	0.1183
P.M.(luminance only)	<b>0.8135</b>	<b>0.8135</b>	<b>0.0333</b>	<b>0.3152</b>
P.M.(color model)	<b>0.8135</b>	<b>0.8135</b>	<b>0.0333</b>	<b>0.4577</b>

of TID2008 and TID2013 show no difference except for the RSC, BRISQUE, and NIQE, which can also be observed in the CSQI database, because one set of the three databases is composed of four or five images. Because the set is composed of such a small number of images, we can observe that the rank estimation is well performed except for the case where the rank estimation does not fit in all the specific sets. However, for the CCID2014 database, the SRCC values of all algorithms are different because the number of images constituting one set of the CCID2014 database is larger. In this experiment, because all the images with contrast changes of one original image are considered as one set, the rank can be further subdivided in the case of the CCID2014 database. Even in this case, we can see that the proposed method shows a higher correlation than the comparison algorithms. This is the same for KRCC, denoted in Table 4, except for RSC, BRISQUE, and NIQE, which show that the existing algorithms differ only in the CCID2014 database. In case of KRCC, RAMMG shows a higher correlation factor than the proposed method, which only uses the luminance component, but the proposed method using a color model shows higher



FIGURE 7. Example of a collected scene for subjective tests.

correlation than other existing IQA methods. Among the existing IQA methods, DIQM has the highest correlation in most databases. Because the proposed method involves computation of the color difference domain, the complexity increases and the computation time becomes longer than that in the DIQM. However, we can see that the proposed method has the same or higher correlation to the DIQM for the three correlation factors.

### C. PERFORMANCE EVALUATION USING SUBJECTIVE TESTS

As mentioned in Sec IV-B, we evaluated the performance of the proposed method using various databases. However, these databases do not fully comply with the meaning of the NR contrast measurement because they are organized as a set. To verify the validity of the proposed method, we proceeded with experiments using subjective tests. We collected various images from still object to outdoor scene using Flickr.com and several image search engines. Fig. 7 shows an example of the collected scene that we used in the experiment.

Using the collected images, we set up the experimental environment to obtain MOS. This experimental environment was set up in a dark room following the ITU-R BT.500-13 guideline [29]. For the experiment, 16 students were assigned. Half of them majored in engineering, and the others were not related to this field. Each experimenter was made aware of the experiment and sample image before measuring MOS. The experiments were performed by scoring one to five points for poor to excellent images for each image. Using these measured MOS, we compare how high the NR contrast measurement methods, including the proposed method, are correlated with MOS. Because this experiment was a measurement for a single image where a reference image did not exist, only PLCC could be applied among the correlation factors presented in Sec. IV-B.

Table 5 lists the correlation factor with MOS from the experiment and measurement methods. We used the same parameters for the proposed methods, and the results of the proposed method and the algorithm with the highest value are shown in bold.

The overall PLCC listed in Table 5 is lower than that from the databases presented in Sec IV-B. This result can be attributed to the differences in the database used in the two



TABLE 5. PLCC of the algorithms using subjective tests.

	PLCC
RMS	<b>0.7412</b>
RME	0.6891
RAMMG	0.6530
DIQM	0.4090
CRME	0.7831
RSC	0.2189
BRISQUE	0.2207
NIQE	0.1803
P.M.(luminance only)	<b>0.8795</b>
P.M.(color model)	<b>0.8827</b>

experiments. In the case of PLCC of Sec. IV-B, because it was an experiment composed of each set, we can observe that the PLCC value is higher than that presented in Sec. IV-C, which uses only one image. Because the number of images is much larger than that in the databases, PLCC is smaller than that in Sec. IV-B. Although the PLCC value listed in Table 5 is smaller than that presented in Sec. IV-B, the PLCC value of the proposed method is the highest among those of the comparison algorithms, which means that the proposed method can reflect the evaluation by people.

## V. CONCLUSION

In this paper, we have proposed the NR contrast measurement method based on HVS. The proposed method consists of measuring the contrast using luminance and chrominance components. The proposed method measures the local contrast of luminance component by JND using the local region background luminance. Moreover, the relationship between brightness and color saturation at V1 is considered in the proposed method to measure the contrast in color difference domain. The experimental results using various datasets and subjective tests show that the proposed method has higher correlation with the people opinion score. As future work, we plan to consider deeper visual stimulus for contrast measurement. We plan to extend this contrast measurement to enhancement applications.

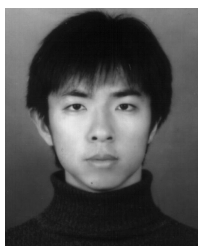
## REFERENCES

- [1] C. Deng, L. Ma, W. Lin, and K. N. Ngan, *Visual Signal Quality Assessment*. Springer, 2016.
- [2] A. M. Eskicioglu and P. S. Fisher, "Image quality measures and their performance," *IEEE Trans. Commun.*, vol. 43, no. 12, pp. 2959–2965, Dec. 1995.
- [3] Z. Wang, A. C. Bovik, H. R. Sheikh, and E. P. Simoncelli, "Image quality assessment: From error visibility to structural similarity," *IEEE Trans. Image Process.*, vol. 13, no. 4, pp. 600–612, Apr. 2004.
- [4] Z. Wang, E. P. Simoncelli, and A. C. Bovik, "Multiscale structural similarity for image quality assessment," in *Proc. 37th Asilomar Conf. Signals, Syst. Comput.*, vol. 2, Nov. 2003, pp. 1398–1402.
- [5] L. Xu, W. Lin, and C.-C. J. Kuo, *Visual Quality Assessment by Machine Learning*. Singapore: Springer, 2015.
- [6] C. Li, A. C. Bovik, and X. Wu, "Blind image quality assessment using a general regression neural network," *IEEE Trans. Neural Netw.*, vol. 22, no. 5, pp. 793–799, May 2011.
- [7] M. Leszczuk et al., "Key indicators for monitoring of audiovisual quality," in *Proc. 22nd Signal Process. Commun. Appl. Conf. (SIU)*, Apr. 2014, pp. 2301–2305.
- [8] K. S. Song, H. Kang, and M. G. Kang, "Contrast enhancement algorithm considering surrounding information by illumination image," *J. Electron. Imag.*, vol. 23, no. 5, pp. 053010, 2014. [Online]. Available: <https://doi.org/10.1117/1.JEI.23.5.053010>
- [9] S. Pan, X. An, and H. He, "Adapting iterative retinex computation for high-dynamic-range tone mapping," *J. Electron. Imag.*, vol. 22, no. 2, p. 023006, 2013. [Online]. Available: <https://doi.org/10.1117/1.JEI.22.2.023006>
- [10] A. Mittal, A. K. Moorthy, and A. C. Bovik, "No-reference image quality assessment in the spatial domain," *IEEE Trans. Image Process.*, vol. 21, no. 12, pp. 4695–4708, Dec. 2012.
- [11] Y. Fang, K. Ma, Z. Wang, W. Lin, Z. Fang, and G. Zhai, "No-reference quality assessment of contrast-distorted images based on natural scene statistics," *IEEE Signal Process. Lett.*, vol. 22, no. 7, pp. 838–842, Jul. 2015.
- [12] A. A. Michelson, *Studies in Optics*. North Chelmsford, MA, USA: Courier Corporation, 1995.
- [13] E. Peli, "Contrast in complex images," *J. Opt. Soc. Amer. A, Opt. Image Sci.*, vol. 7, no. 10, pp. 2032–2040, Oct. 1990. [Online]. Available: <http://josaa.osa.org/abstract.cfm?URI=josaa-7-10-2032>
- [14] S. S. Agaian, "Visual morphology," *Proc. SPIE*, vol. 3646, pp. 3646-1–3646-12, Mar. 1999. [Online]. Available: <https://doi.org/10.1117/12.341081>
- [15] K. Panetta, C. Gao, and S. Agaian, "No reference color image contrast and quality measures," *IEEE Trans. Consum. Electron.*, vol. 59, no. 3, pp. 643–651, Aug. 2013.
- [16] K. Panetta, L. Bao, and S. Agaian, "A human visual 'no-reference' image quality measure," *IEEE Instrum. Meas. Mag.*, vol. 19, no. 3, pp. 34–38, Jun. 2016.
- [17] L. M. Hurvich and D. Jameson, "An opponent-process theory of color vision," *Psychol. Rev.*, vol. 64, no. 6p1, p. 384, 1957.
- [18] E. N. Johnson, M. J. Hawken, and R. Shapley, "The orientation selectivity of color-responsive neurons in macaque V1," *J. Neurosci.*, vol. 28, no. 32, pp. 8096–8106, 2008. [Online]. Available: <http://www.jneurosci.org/content/28/32/8096>
- [19] D. Xing, A. Ouni, S. Chen, H. Sahnoud, J. Gordon, and R. Shapley, "Brightness–color interactions in human early visual cortex," *J. Neurosci.*, vol. 35, no. 5, pp. 2226–2232, 2015. [Online]. Available: <http://www.jneurosci.org/content/35/5/2226>
- [20] C.-H. Chou and Y.-C. Li, "A perceptually tuned subband image coder based on the measure of just-noticeable-distortion profile," *IEEE Trans. Circuits Syst. Video Technol.*, vol. 5, no. 6, pp. 467–476, Dec. 1995.
- [21] W. M. Morrow, R. B. Paranjape, R. M. Rangayyan, and J. E. L. Desautels, "Region-based contrast enhancement of mammograms," *IEEE Trans. Med. Imag.*, vol. 11, no. 3, pp. 392–406, Sep. 1992.
- [22] A. Rizzi, T. Algeri, G. Medeghini, and D. Marini, "A proposal for contrast measure in digital images," in *Proc. Conf. Colour Graph., Imag., Vis.*, 2004, pp. 187–192.
- [23] A. Rizzi, G. Simone, and R. Cordone, "A modified algorithm for perceived contrast measure in digital images," in *Proc. Conf. Colour Graph., Imag., Vis.*, 2008, pp. 249–252.
- [24] M. Kim, K. S. Song, and M. G. Kang, "No-reference image contrast assessment based on just-noticeable-difference," *Electron. Imag.*, vol. 2017, no. 12, pp. 26–29, 2017.
- [25] N. Ponomarenko et al., "TID2008-A database for evaluation of full-reference visual quality assessment metrics," *Adv. Mod. Radioelectron.*, vol. 10, no. 4, pp. 30–45, 2009.
- [26] N. Ponomarenko et al., "Image database TID2013: Peculiarities, results and perspectives," *Signal Process., Image Commun.*, vol. 30, pp. 57–77, Jan. 2015.
- [27] E. C. Larson and D. M. Chandler, "Most apparent distortion: Full-reference image quality assessment and the role of strategy," *J. Electron. Imag.*, vol. 19, no. 1, p. 011006, 2010. [Online]. Available: <https://doi.org/10.1117/1.3267105>
- [28] K. Gu, G. Zhai, W. Lin, and M. Liu, "The analysis of image contrast: From quality assessment to automatic enhancement," *IEEE Trans. Cybern.*, vol. 46, no. 1, pp. 284–297, Jan. 2016.
- [29] *Methodology for the Subjective Assessment of the Quality of Television Pictures*, Standard ITU-R BT.500-11, 2003.
- [30] L. I.-K. Lin, "A concordance correlation coefficient to evaluate reproducibility," *Biometrics*, vol. 45, no. 1, pp. 255–268, 1989.
- [31] J. B. Carroll, "The nature of the data, or how to choose a correlation coefficient," *Psychometrika*, vol. 26, no. 4, pp. 347–372, 1961.
- [32] M. G. Kendall, A. Stuart, and J. K. Ord, *The Advanced Theory of Statistics*, vol. 1. London, U.K.: Griffin, 1948.
- [33] A. Mittal, R. Soundararajan, and A. C. Bovik, "Making a 'completely blind' image quality analyzer," *IEEE Signal Process. Lett.*, vol. 20, no. 3, pp. 209–212, Mar. 2013.



**MINSUB KIM** received the B.S. degree in electronics engineering from Yonsei University, Seoul, South Korea, in 2014, where he is currently pursuing the Ph.D. degree with the Department of Electrical and Electronic Engineering.

His current research interests include contrast enhancement and image quality assessment based on the human visual system.



**KI SUN SONG** received the B.S. and Ph.D. degrees in electrical and electronic engineering from Yonsei University, Seoul, South Korea, in 2009 and 2017, respectively. He is currently a Post-Doctoral Researcher with the Department of Electrical and Electronic Engineering, Yonsei University.

His current research interests include image enhancement, dynamic range compression, image filtering, and high dynamic range.



**MOON GI KANG** received the B.S. and M.S. degrees in electronics engineering from Seoul National University, Seoul, South Korea, in 1986 and 1988, respectively, and the Ph.D. degree in electrical engineering from Northwestern University, Evanston, IL, USA, in 1994.

He was an Assistant Professor with the University of Minnesota, Duluth, MN, USA, from 1994 to 1997, and since 1997, he has been with the Department of Electronic Engineering, Yonsei University, Seoul, where he is currently a Professor. He has authored over 100 Technical articles in his areas of expertise. His current research interests include image and video filtering, restoration, enhancement, and superresolution reconstruction. He served as the Editorial Board Member for the *IEEE Signal Processing Magazine*, the Editor of SPIE Milestone Series Volume (CCD and CMOS imagers), and the Guest Editor of the *IEEE Signal Processing Magazine* Special Issue on Superresolution Image Reconstruction (May 2003). He has served in the technical program and steering committees of several international conferences. He has also served as the Associate Editor of the *EURASIP Journal of Advances in Signal Processing* and the Associate Editor of the *Digital Signal Processing* in Elsevier Journal. He was a recipient of 2006, 2007, and 2012 Yonsei Outstanding Research Achievement Awards (Technology Transfer), the 2002 HaeDong Foundation Best Paper Award, and the 2000, 2009, and 2010 Awards of Teaching Excellence at Yonsei University.

...